ELSEVIER

Journal of Neuroscience Methods 115 (2002) 189–198

JOURNAL OF NEUROSCIENCE METHODS

www.elsevier.com/locate/jneumeth

Accurate quantitative RT-PCR for relative expression of *Slo* splice variants

Sahar F. Mahmoud, Alex L. Bezzerides, Rebecca Riba, Guey-Jen Lai, Peter V. Lovell, Yuko Hara, David P. McCobb *

Department of Neurobiology and Behavior, Cornell University, W153 Mudd Hall, Ithaca, NY 14853, USA

Received 11 October 2001; received in revised form 22 January 2002; accepted 22 January 2002

Abstract

Much interest has been shown in the use of multi-template reverse transcription-polymerase chain reaction (RT-PCR) as a quantitative instrument for low-abundance mRNAs. A desire to achieve finely-graded quantification of the stress- and hormone-related regulation of one splicing decision in an ion channel gene motivated us to test the reliability of simultaneous amplification of two splice variants with one pair of flanking constitutive primers. Unexpectedly indiscriminate heteroduplexing between the two amplification products, despite a large length difference, and their tight comigration with one homoduplex, mandated a rigorously-denaturing electrophoresis protocol. Conveniently, a new fluorescent dye with high affinity for single-stranded DNA has become available. Though the dye has a good dynamic range, we found that dye and gel saturation compounded by the length difference between products introduced an asymmetrical error into the calculation of relative abundance. Avoiding several pitfalls, dye calibration could be used to correct the error. We also found that differences in the amplification efficiency of the two templates were not constant, but dependent on the initial template ratio, requiring a non-linear correction. Together these improvements gave us very consistent quantitative results, and thus advance our analysis of hormonal mechanisms underlying the regulation of alternative splicing of an ion channel critically involved in stress responses.

Keywords: Competitive RT-PCR; Denaturing gel electrophoresis; SYBR Gold; Slo; Alternative splice variants

1. Introduction

As a complete list of genes encoding proteins approaches realization, the challenges of quantifying their expression patterns in space and time become paramount. This is particularly apparent in the nervous system, where diverse technical innovations and refinements will clearly be needed to approach such nano-enigmas as everyday information storage in the brain. The ability of reverse transcription-polymerase chain reaction technology (RT-PCR) to detect a very few copies of a grossly outnumbered RNA species is widely exploited. A number of labs have tested and expanded the potential of RT-PCR as a quantitative instrument, particularly through calibration with a specifically engineered exogenous co-template (Diviacco et al., 1992; Apostolakos et al., 1993; McCulloch et al., 1995; Hayward et al., 1998; Vu et al., 2000). These studies favor avoiding co-templates that amplify with different efficiencies, an unavoidable situation for our purposes. Innovations involving real-time monitoring of fluorescence changes during amplification also improve prospects for quantification, but come with their own complications, and require special equipment and technical skills that are not now widely available (Bustin, 2000; Jung et al., 2000).

Our interest was in accurately determining the relative abundance of a pair of splice variants with an inherent and sizable length difference. Just these two of several possible splicing configurations in one stretch of the *Slo* gene are expressed in significant abundance in rat adrenal medulla (Xie and McCobb, 1998). The gene encodes calcium- and voltage-gated potassium channels ('BK') that help shape the electrical excitability of diverse cell types, from auditory hair cells to vascular

* Corresponding author. Tel.: +1-607-254-4321; fax: +1-607-254-4308.

E-mail address: dpm9@cornell.edu (D.P. McCobb).

0165-0270/02/$ - see front matter
PII: S0165-0270(02)00015-8

and intestinal smooth muscle cells (Brenner et al., 2000; Meera et al., 2001; McCobb, 2002). RT-PCR was used previously on rat adrenal medullary tissue to show that the relative abundance of these forms, with and without the 174 base pair 'STREX' exon (for STRess-axis regulated EXon), is sharply altered by pituitary ablation, unless accompanied by adrenocorticotropic hormone (ACTH) replacement (Xie and McCobb, 1998). This finding is interesting both mechanistically and in the broader context of vertebrate stress responses. Thus the roles of calcium and kinases, exonic and intronic sequences in the gene (Xie and Black, 2001), pituitary, adrenal, and gonadal hormones, and behavioral and physiological stressors in regulating splicing are all now under investigation (Lai and McCobb, 2001, 2002; Mahmoud et al., 2002). The choice of exon configuration robustly affects channel gating (Saito et al., 1997; Xie and McCobb, 1998; Ramanathan et al., 1999) and responses to protein kinase A (PKA) phosphorylation (Tian et al., 2001). Moreover, hormonal regulation of the splicing event in adrenal medulla has been shown to contribute to pituitary-mediated tuning of the electrical excitability of catecholamine-secreting chromaffin cells (Lovell and McCobb, 2001).

The RT-PCR approach used previously was adapted from 'competitive' or 'calibrated' PCR, on the simple assumption that the splice variants could replace exogenous calibration templates, serving as 'built-in' internal standards for measuring the abundance of each relative to the other. Thus a single primer pair was used to amplify the two templates, with the products then distinguished by their electrophoretic mobility. In the original observation, RT-PCR products were run on 2% agarose gels, and the two prominent bands were identified as STREX and ZERO (having no optional insert at this splice site) variants of Slo. A slower running third band that was attributed to heteroduplex formation between STREX and ZERO was occasionally observed, but could be consistently avoided by holding at 72 °C for 15 min immediately after the final denaturation step. We have since discovered that an additional heteroduplex band was overlooked because it migrated at a rate nearly identical to that of the STREX product. Though others have identified and quantified similar heteroduplexes between related amplicons (McCulloch et al., 1995; Hayward et al., 1998; Serth et al., 1998; Vu et al., 2000), we were concerned about variability in its formation and complexity in its quantification on gels. Motivated to maximize the measurement accuracy of Slo splice variant expression to better understand its regulation, we explored the limits of this multi-product RT-PCR approach in several respects.

2. Materials and methods

Choice of primer pair for two-template PCR reactions is critical, since the primers define the length of both products and the proportionate difference between the two lengths. The length difference must be great enough to enable clean electrophoretic separation, but small enough that relative amplification efficiencies, and thus product amounts (or detection sensitivities) are similar. PCR primers RbSlo1 5′AGTGCCTTCGTGGGCTGTCCTTC 3′ and QRA59 5′ CACATTGGAGTCCATGTTGTC 3′ were selected over other primers on a trial and error basis (Fig. 1A). Separate STREX and ZERO templates for test reactions were obtained from cDNA plasmids developed for *Xenopus* oocyte expression (Xie and McCobb, 1998). Large stocks of these amplicons were generated for use in gel calibration and as test templates. DNA concentrations were initially estimated spectrophotometrically and fluorometrically in solution, and refined by electrophoresing several series of dilutions alongside the Bio-rad Precision Mass Ruler, with careful consideration for the dye saturation related issues discussed in Section 3. Dilutions (and pre-mixes of STREX and ZERO templates for amplification efficiency calibration) were done by weight using an analytical balance and a micropiper, assuming solution densities of 1 g/ml.

PCR reactions were 25 μl, with standard PCR buffer (Promega, 1.5 mM $MgCl_2$), 0.2 mM each dNTP, and 0.125 μl Taq polymerase. After 3 min at 95 °C, reactions were cycled for 30 s each at 94, 55, and 72 °C. PCR products were run on 2% or 3.5% agarose with 0.5× Tris Borate EDTA buffer (TBE, Sigma), post-stained with ethidium bromide for 30 min, destained for 15 min, and digital images acquired with an LG-3 digitizer and modified NIH Image software (version 1.62, Scion Corp.). Our best denaturing agarose gels were made and run in the vertical gel casting system designed for PAGE gels (Bio-Rad), with 2% agarose, 40% formamide and 5% formaldehyde. To test the 120 ml chamber of running buffer, 20 ml of formamide was also added. After post-staining with SYBR Gold (Molecular Probes, Eugene, OR), images were captured with the STORM Imager (Molecular Dynamics) or with the Scion acquisition system described in results. Denaturing PAGE gels were made and treated as described in Section 3. Silver staining was done with a kit from Promega initially, but off-the-shelf reagents were substituted without detriment.

Gel band densitometry was done initially with the 'Gel Plotting Macro' available with Scion Image, or with the similar 'Band-Buster' software, an Igor (Wavemetrics, Lake Oswego, OR) procedure developed in-house (PVL and DPM, contact DPM for further information). Both procedures plotted a 'vertical profile', a graph plotting vertical position on the gel lane on

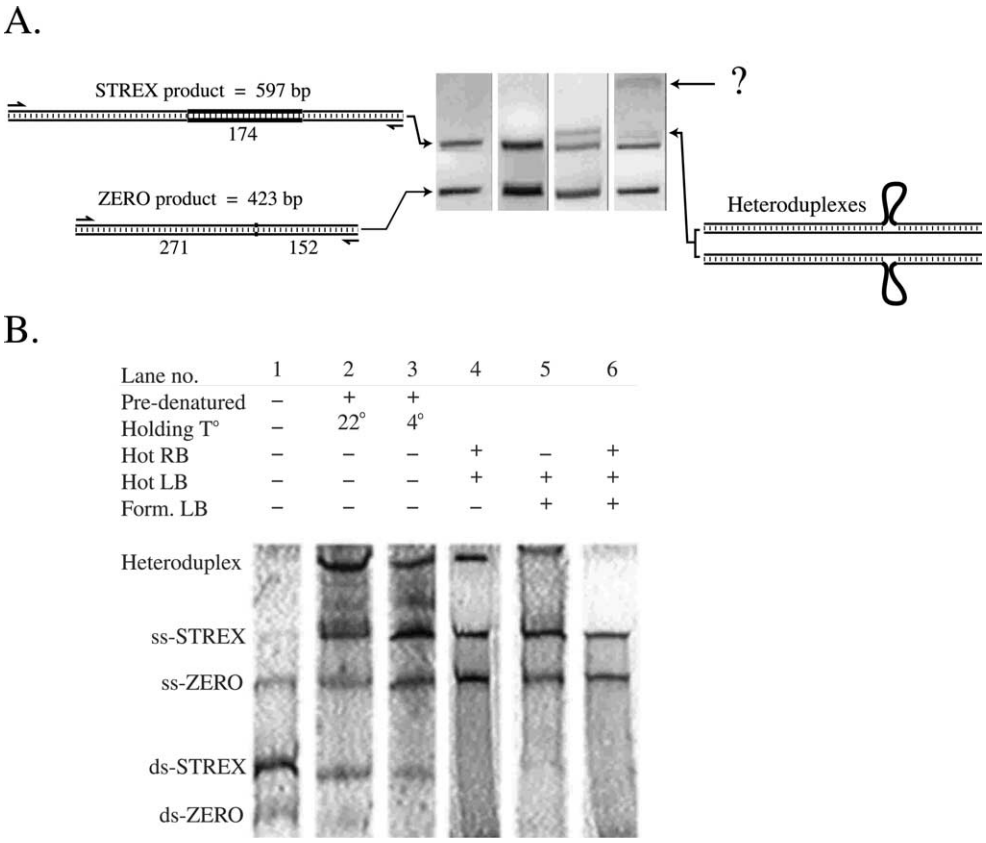

Fig. 1. (A) PCR products with and without the 174 bp STREX exon generated from the *Slo* gene using primers RbSlo1 and QRA59. Lane 1 shows STREX and ZERO products generated separately and combined just before running on a 2% agarose gel. In lanes 2–4, STREX and ZERO products were denatured, and allowed to reanneal in the same tube. What looks like two bands on a 2% agarose gel (Lane 2) can be resolved into three or four bands (Lanes 3 and 4, respectively) on a 3.5% gel. (B) Lanes from silver-stained denaturing PAGE gels containing 40% formamide by volume. Lane 1, products not denatured together before running. Note both double-stranded (ds) and single-stranded (ss) products are detectable, but heteroduplex is absent (heteroduplex runs much more slowly in PAGE gels, and some portion often remains in the wells, making it unquantifiable). In the remaining lanes, products were denatured by boiling for 2 min and run after being held briefly at room temperature, 4 °C, or ~98 °C. The only combination of conditions that worked reliably was to have 40% formamide in the loading buffer (Form. LB) as well as the gel, and to maintain both the loading buffer and the running buffer (RB) at near boiling temperature.

the abscissa against the sum of horizontal grayscale values for each row of pixels on the ordinate. Background subtraction was accomplished by drawing a baseline connecting background values on either side of the band peak, and integrating the area between the baseline and the peak profile. Band-Buster had the advantage that integrated areas were not scaled to arbitrary working dimensions, which allowed direct comparisons of measured values across similarly treated gels, and also automated the calibration and data handling processes.

For experiments on animal tissues, tissues were dissected as described previously (Xie and McCobb, 1998) and quick-frozen on dry ice. Total RNA was extracted using the Qiagen RNeasy kit, and 2 μg of RNA was used in a 20 μl reverse transcription reaction primed with oligo d(T). Two μl of the RT product was added to each PCR reactions. Negative controls (no template) were run in parallel.

To minimize the number of data points needed to approximate the exponential dye saturation function, plots of band intensity as a function of absolute DNA amount in standards were constrained through zero using the single exponential equation, $Y = A*(1-\exp(-B*X))$, where Y = fluorescence signal and X = DNA in ng. Correction for the dependence of amplification efficiency on starting template ratio was done by fitting STREX fraction in the product vs. template with a modified Boltzmann function, as described in Section 3.

3. Results

3.1. Heteroduplex DNA

Interest in hormonal and experience-related regulation of alternative splicing of the *Slo* gene prompted a critical investigation of a 'competitive' RT-PCR ap-

proach to determining the relative abundance of two splice variants. We have established that only forms with and without the 174 bp STREX exon occur in significant abundance in rat adrenal medulla tissue (Xie and McCobb, 1998). However, though the products generated with primers targeting the constitutive flanking exons appear on a 2% agarose gel to be two distinct and homogenous bands, we can now resolve them into three prominent bands by running at least 4 cm on a 3.5% agarose gel (Fig. 1A). Repeated attempts to subclone the top band to identify other variants yielded STREX and ZERO clones but no new sequences. Instead we found that an identical band could be generated from mixes of pure STREX and ZERO PCR products (from plasmid clones) by simply denaturing the mix and allowing reannealing. This band thus constitutes heteroduplexing between sense and antisense strands of STREX and ZERO products, which share 423 bp of sequence, with the 174 bp STREX exon itself apparently looping out and slowing migration only slightly relative to the STREX homoduplex.

Others have found heteroduplexing either to be a minor component in cases with substantial internal sequence disparity, or to be adequately separable and quantifiable (McCulloch et al., 1995; Hayward et al., 1998; Serth et al., 1998; Vu et al., 2000). We found it impossible to eliminate heteroduplexing between STREX and ZERO. We tried a wide variety of temperature and buffer protocols to achieve selective homoduplexing of STREX and ZERO strands. Protocols ranged from a slow ramp cooling from 95 to 4 °C, to long dwell times at a wide range of intermediate temperatures. Cooling to 4 °C either too fast, or not at all, resulted in substantial non-reannealing. Cooling at intermediate dwell temperatures invariably gave the primary heteroduplex band, and at most temperatures, one or two additional bands, perhaps representing three strand configurations similar to Holliday junctions, or other tertiary structures (Yakubovskaya et al., 2001). Reannealing at 72 °C for 30 min following denaturation and then immediately loading and running samples was the only way to consistently avoid getting more than three bands.

To estimate the extent and quantifiability of heteroduplexing, we made a series of mixes with varying ratios of STREX and ZERO PCR products, denatured them at 95 °C for 3 min, and reannealed them at 72 °C for 30 min. We then quantified the intensities of the three bands in each lane, and corrected raw intensity values for length differences to estimate relative copy numbers. STREX intensities were multiplied by 0.709 to compensate for the longer length of STREX relative to ZERO products. Heteroduplex band intensities were not adjusted, on the assumption that ethidium binding to the single-stranded loop of the STREX exon would be negligible. The simplest possible probabilistic model of the duplexing process gave a good approximation of experimental results (Fig. 1B). If duplexing were totally indiscriminate, i.e. a single STREX strand (s) would be as likely to duplex with the complementary strand of ZERO (z) as with its full-length complement, the following equations could be used to calculate the proportions of homo- and heteroduplexes that should form from a known mix of STREX and ZERO. S (upper case) represents the proportion of starting material that is STREX, whereas ss and zz (lower case) represent the proportions of the post-annealing mix that are homoduplexed STREX and ZERO, respectively. The remaining duplex DNA would be of two forms sz and zs, and the sum of $ss+zz+sz+zs=1$. From simple probabilities, the proportion of homoduplexes would be; $ss=S^2$ and $zz=(1-S)^2$. The sum of the heteroduplexes would then be; $(sz+zs)=1-(S^2)-(1-S)^2$. To test this model, we ran four copies of the full series of both non-denatured and denatured and reannealed DNA out on 3.5% agarose gels. Copy number estimates of ss, zz, and heteroduplex strands conformed quite well to the pattern predicted (Fig. 1B), except that the heteroduplex fraction peaked at roughly 0.4 rather than 0.5, with the proportions of ss and zz strands correspondingly elevated. The data were well fit by a single-term polynomial where $ss=aS^2$, $zz=b(1-S)^2$, and heteroduplex $=1-(ss+zz)$. Coefficients a and b were 1.02 and 1.21, respectively. The difference between these constants may represent different binding affinities of different strand combinations, inequities in staining or quantification of bands, or other measurement error. The results indicate that the annealing of STREX and ZERO is remarkably indiscriminate, considering that the length of the non-annealing loop of STREX is 41% of the length of shared sequence. To determine whether data collected without resolving STREX homoduplex (ss) from heteroduplex could be used to estimate S, we consulted the model. Fig. 2B shows a plot of the sum of $ss+(sz+zs)$ as it varies over the full range of S values (from 0 to 1). Though in principle one can back-extrapolate from any value of the sum to a corresponding value of S, this would be particularly imprecise on the high end of the range, since minimal changes in intensities of the two bands would imply large changes in S.

We found that reasonable estimates of S in unknowns could be made by running samples on non-denaturing agarose gels and simply adding half the heteroduplex value to each of the ss (already length-corrected) and zz values. Such estimates were reproducible. However, estimates were unsatisfactory if annealing conditions permitted the formation of more than the three bands in the gel.

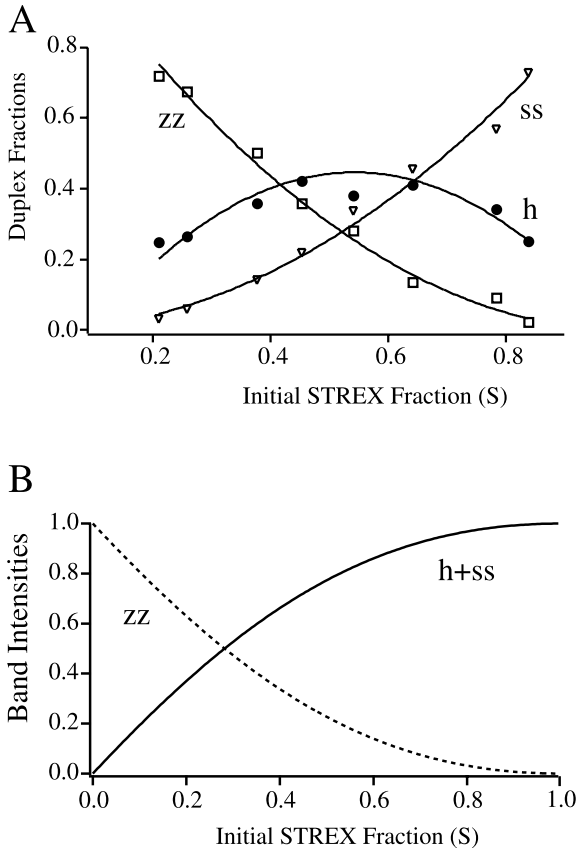

Fig. 2. (A) Heteroduplexes (h) form with almost as high a probability as STREX and ZERO homoduplexes (ss and zz, respectively). The two homoduplexes were mixed to give various initial STREX fractions, and the mixes were heat denatured and reannealed at 72 °C for 30 min before loading on a 3.5% agarose gel. The fraction of the total strand number that ended up in homo- and heteroduplexes was then determined by measuring the fluorescence of the three bands and correcting for length differences. With an initial STREX fraction of 0.5, random reannealing would result in half of the DNA to end up as heteroduplex. The actual rate was only slightly lower than that, despite the 174 bp intervening sequence that was not shared. (B) The theoretical proportion of strands ending up in the ZERO band and a non-resolved STREX+heteroduplex band for various initial STREX fractions.

3.2. Denaturation, detection, and quantification

Denaturing gel electrophoresis, if reliably complete, could eliminate heteroduplex concerns. Using silver staining to visualize single stranded DNA, we found that ensuring full denaturation without secondary structure was not easily achieved. As summarized in Fig. 2, unacceptable levels of duplexing can occur under all but the most stringent conditions. Urea is commonly used in denaturing PAGE gels for DNA. We obtained more consistent results with formamide (40% by volume in 8% PAGE gels, acrylamide:bis-acrylamide ratio = 19:1). Adding urea in addition to formamide did not improve denaturation, and sometimes gave undesirably cigar-shaped bands. After experimenting widely with loading buffer composition, we concluded that the best results were obtained with formamide comprising 80% (by volume) of the 2× loading buffer, which also contained 20 mM EDTA and 10% sucrose (EDTA and sucrose were first dissolved in the water that comprised 20% of the final volume). The width of DNA bands in the gel lanes was found to be quite sensitive to total loading volume (but not ionic strength or formamide amount), and because dye saturation (see below) is affected by band width, water was added to equalize sample volumes before adding equal volumes of the 2× loading buffer. Importantly, no gel or loading buffer combinations could guarantee full denaturation. Thus we boiled samples for 1 min in an electric pot after adding the loading buffer, and left them in the near boiling water until individually loaded. Even when immersed immediately in ice water significant reannealing could take place after boiling. Moreover, to reliably eliminate duplexing we found it necessary to heat the running buffer to boiling temperature just before pouring it into the gel box and loading samples. Denaturing agarose gels proved feasible, as described in Section 2, but somewhat less consistent than PAGE, in part because they could not be run hot.

3.3. Gold over silver

Ethidium bromide has a very low affinity for single stranded DNA. Silver staining is at least 100 times more sensitive, and offers a convenient alternative to radioisotopes (Gottlieb and Chavko, 1987). Excellent images can be made of silver stained gels by laying the gel directly on an inexpensive digital scanner equipped with a transparency adapter (e.g. Epson Perfection 1200U). However, for quantification, the dynamic range of staining intensity was narrow, and developing the gel to the right intensity, necessarily by eye, too crude. SYBR Gold is a fluorescent dye that binds to single-stranded DNA with sufficient affinity to detect sub-nanogram amounts (Tuma et al., 1999). A standard UV transilluminator can be used to illuminate the gel, and a band pass filter available from Chroma (Brattleboro, VT) passes the 535±20 nm dye-emission, while very effectively eliminating UV excitation and infrared background radiation. (A single filter that works with both ethidium bromide and SYBR Gold is in development). A digital image acquisition system with on-chip integration controlled with NIH-Image software maximizes dye-detection sensitivity at minimal cost (Scion Corp., Frederick, MD). Pixel intensity depth of 8-bit (256 grayscale values) is minimal, and requires care to avoid saturation on either end. Color digital cameras costing under $1000 with 12-bit depth (4096 values) per color channel, used directly with long exposure times, offer a better dynamic range, and 12-bit monochrome cameras

designed for scientific applications, with high sensitivity and low noise, are becoming more affordable.

SYBR Gold can also be imaged with a Molecular Dynamics 'STORM' imager (Sunnyvale, CA), which has a wide dynamic range. We used STORM to test for saturation and resultant non-linearity in our gel bands. As shown in Fig. 3, dye emission from gel bands on a 1 mm thick PAGE gel can exhibit non-linearity within the desirable working range. This apparent saturation is partly the result of fluorescence concentration quenching, also referred to as the inner-filter effect (Ingle and Crouch, 1988; Mahmoud, 1994). Since there is overlap between the absorption and emission spectra of SYBR Gold, some of the emitted photons will be reabsorbed by the dye, causing self-quenching. Gel overloading can contribute as well. Particularly with PAGE gels, exceeding the capacity of the lane results in a smear of DNA stretching beyond the lower boundary of the band, some of it far beyond. This necessitates delimiting the peak in the profile plot with a slanted baseline, and discounting some smeared DNA. Though increasing gel thickness increases dye 'stacking' in the thickness dimension, which is responsible for some saturation, in our hands, the increased capacity of a 1.5 mm thick gel over a 1 mm thick gel more than offsets the increase in thickness.

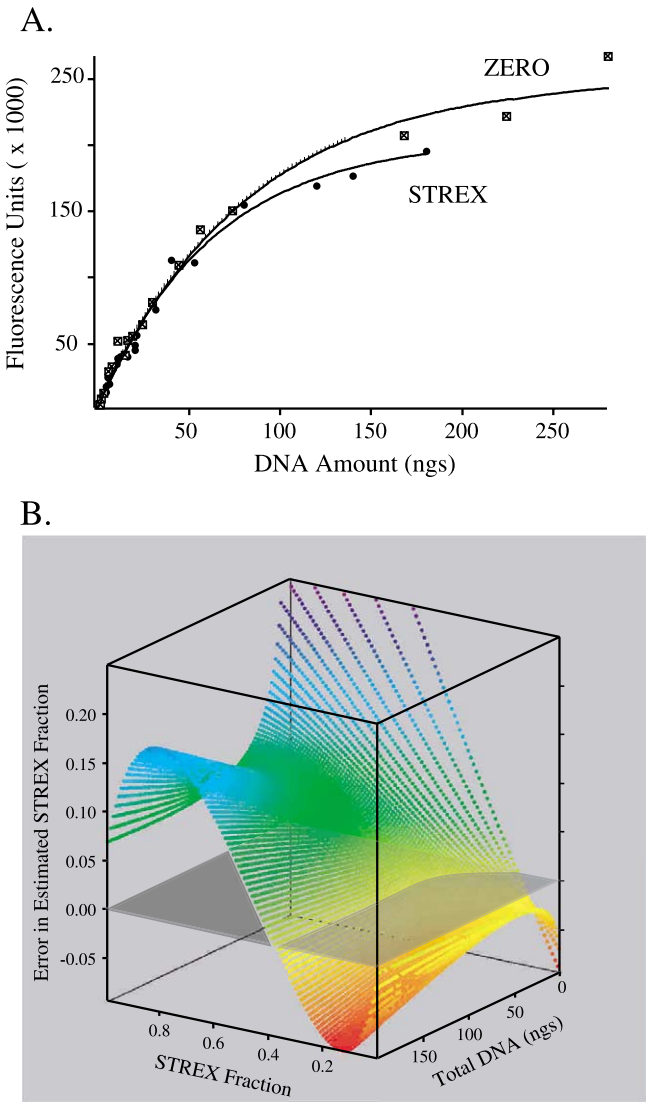

Fig. 3. (A) Fluorescence signal from predetermined amounts of STREX and ZERO products on a 1 mm thick PAGE gel stained with SYBR Gold. Fits are unconstrained exponential fits. (B) Error in the estimated STREX fraction that would result from failure to take into account the exponential dye saturation shown in A. The asymmetry, including the fact that the error passes through zero at a STREX fraction of approximately 0.4 rather than 0.5, derives mostly from the difference in copy number for equal absolute amounts of DNA for the two products.

Though saturation on a 1 mm gel is not severe below 100 ng of DNA, working with PCR products with unknown DNA concentrations that might vary widely in the proportions of two products (STREX vs. ZERO, in our case), make it necessary to take saturation into account. STREX and ZERO show somewhat different saturation profiles, consistently, because ZERO, by running further, spreads a bit more on the gel and the dye is, therefore, less concentrated. This inequity will bias the estimated ratio of the two products. However, the situation is compounded much more by our interest in copy number, as opposed to DNA amount. Thus STREX, being 41% longer, requires that much more DNA to achieve the same copy number. Fig. 3B illustrates the error in the estimated STREX fraction (in copy number) associated with failure to take dye saturation into account. The error was calculated from the exponential fits shown in A, and varies asymmetrically for both of the aforementioned reasons.

We found lane width to be surprisingly sensitive to loaded volume, with little dependence on loading buffer composition. Moreover, dye saturation was demonstrably worse with narrower lanes (as well as shorter running distances). Standardization of loading volume eliminated the problem for all but the outside lanes, which were consistently narrower than the rest.

Avoiding lane width and overloading problems, dye saturation error can be corrected for very effectively by calibrating gels with premeasured STREX and ZERO DNA standards. Data like that in Fig. 3A were consistently well-fit by a single exponential, and unconstrained fits passed very close to the origin. This is consistent with the inherently low background in SYBR Gold stained gels, and the high sensitivity and near linear behavior in the low range. These results permit a reproducible reconstitution of the saturation function from three or four calibration standards, using a fitting equation constrained to pass through the origin (see Section 2). We obtained very reproducible fit parameters running, respectively, 10, 33, and 100 ng of STREX in three lanes, and 140, 47, and 13 ng of ZERO in the same three lanes. These standards were designed to cover the

range of STREX fractions, as well as DNA amounts, occurring in our unknowns, and thus can be used to check the consistency of the fraction estimate. Two gels (ten lanes each) could be run, stained, and calibrated together as a unit, maximizing the number of lanes available for unknown samples, as compared with calibration standards. Running fresh gels at 24 V/cm for 80 min, staining with SYBR Gold, and quantifying in consistent fashion, gave results that were more reproducible, in absolute terms, than can be achieved with silver staining, or with radioisotopes, which are subject to continual decay (Tuma et al., 1999).

3.4. Extrapolating from product ratio to template ratio

To estimate the relative abundance of STREX and ZERO splice forms in the template rather than the product, bias introduced by differences in amplification efficiency of the two templates had to be considered. We devised a cDNA plasmid having both ZERO and STREX templates in it so that we could ensure a starting ratio of 1:1 (Xie and McCobb, 1998). After 30 cycles, the STREX fraction was 0.39, rather than 0.5 (STREX amplification of 78% relative to ZERO). We found 30 cycles to be well within the approximately linear phase of the reaction, with the measured STREX fraction very consistent for cycle numbers up to 38 cycles. The measure was also very robust to variation over five orders of magnitude in the amount of the plasmid template put into the reaction. Finally, rather than assume the relative efficiency was constant across the range of STREX fraction in the template, we made a series of templates varying across the range, ran the 30 cycle reaction, and quantified both template and product mixes identically on a series of calibrated gels. The results with the STREX template at 0.5 were very similar to those obtained with the aforementioned plasmid, but the relative efficiency varied with the STREX fraction, as shown in Fig. 4. The experiment was run three times, with varying ranges of absolute template and product amounts. Despite this variation, data from the three sets demonstrate a consistent relationship between the product STREX fraction and the template STREX fraction (Fig. 4A). The data were well described by a Boltzmann fit of the form, $Y = A/(1+\exp(-B^*(X-C)))+D$, where Y and X are the STREX fractions in product and template, respectively. Thus estimates of template proportions in unknowns can be readily obtained by back-calculating using these pre-determined fit parameters.

3.5. STREX estimates from native tissues

To estimate measurement error in the RT-PCR process, ten small pieces from a single bovine adrenal medulla were processed independently through the entire process from RNA extraction through PCR (Fig. 5A). The independent estimates of template STREX fraction ranged from 0.149 to 0.206, with a mean and standard deviation (S.D.) of 0.187 ± 0.02 (i.e. the S.D. is 11% of the mean value, and 2% of the full range of possible STREX fractions). This represents a very high level of reproducibility, allowing small but consistent differences to be analyzed statistically with modest sample sizes.

Combining all of the above methods, we measured the relative abundance of STREX in an assortment of tissues to get an estimate of naturally occurring variation. As shown in Fig. 5B, adrenal medullae from a cohort of male rats had STREX fractions of approximately 0.4 in both adrenal and pituitary glands, with inter-individual variation over a range of approximately $\pm 5\%$. Rerunning stored RT-PCR products from previously published experiments (Xie and McCobb, 1998)

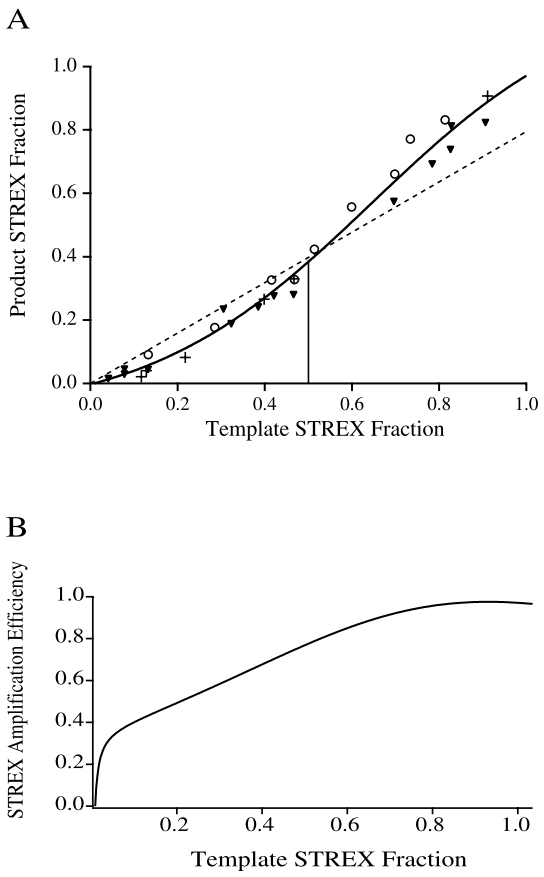

Fig. 4. (A) The relationship between starting template fraction and product fraction for three separate experiments, indicated with three different symbols. The solid curve represents a Boltzmann fit to the data, as described above. Dotted line represents the product fraction expected if the STREX amplification efficiency were a constant 0.78 (relative to ZERO), as was measured with a template STREX fraction of 0.5. (B) STREX amplification efficiency as a function of the template STREX fraction.

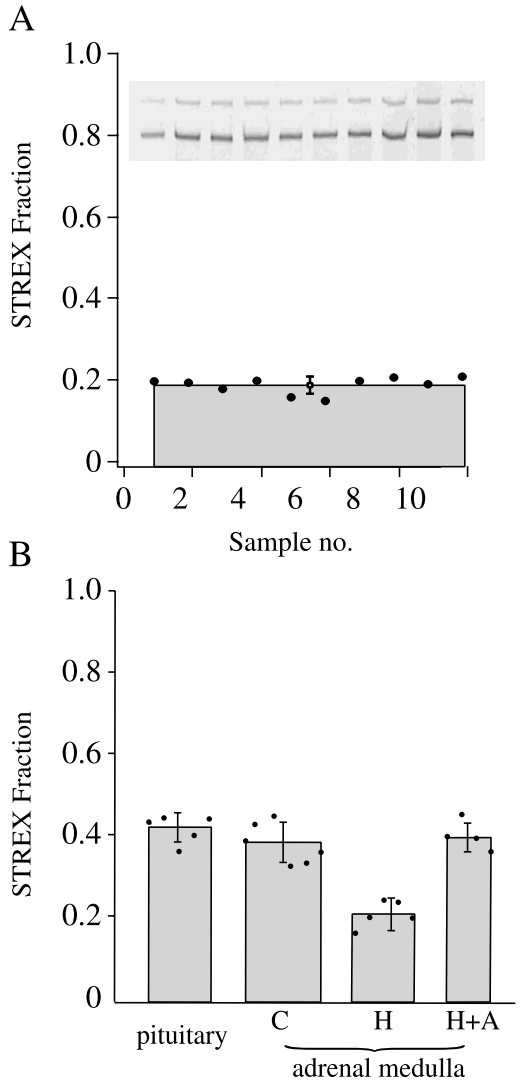

Fig. 5. (A) Ten independent RT-PCR estimates from ten pieces from a single bovine adrenal medulla, showing the very high reproducibility of the result. The S.D. for the STREX fraction is 0.0268. (B) Rat pituitary and adrenal medulla have similar STREX fractions, with inter-individual variation greater than can be attributed to variation in the reaction or measurement error. Hypophysectomy reduces STREX in adrenal medulla by approximately 50%, as compared with 40% from earlier estimates. N, H, and H+A represent normal, hypophysectomized, and hypophysectomized plus ACTH injected rats.

yielded values of 0.39 and 0.40 for two normal male rats, as compared with 0.2 ± 0.04 (mean $\pm$ S.D., $N = 5$) for hypophysectomized rats at 15 days after surgery, and 0.4 ± 0.04 ($N = 4$) for hypophysectomized rats treated with adrenocorticotropic hormone (H+ACTH). One-way ANOVA was used to compare treatment groups. The STREX fraction in adrenals from hypophysectomized rats was significantly lower than normal or hypox+ACTH rats, whether compared in raw intensity values or the more-derived estimates of the STREX template ratio. For the latter, the probability that hypox animals are not different is less than 0.01 (i.e. the family error rate, as determined with Tukey's post-hoc comparison). We, therefore, consider the previously published estimates (0.53, 0.32, and 0.54 for normal, hypox, and H+ACTH rats) to be overestimates, but not grossly different from the improved estimates. This reflects the robustness of the effect of hypophysectomy and ACTH on splicing, but is also partly fortuitous, since some of the error associated with non-separation of heteroduplex from STREX DNA in the unknowns was offset by similarly erroneous calibration of the amplification efficiency, done in parallel using the double plasmid template.

4. Discussion

Simultaneous PCR amplification of two or more templates in a single tube is done both deliberately and unwittingly for various reasons. Spurious bands that are difficult to explain often appear on gels from even straightforward reactions, and the problem is much worse for intentionally compound reactions. We discovered a duplicity arising from the tight co-migration of heteroduplexed STREX and ZERO PCR product with the STREX homoduplex, despite the 174 bp non-shared STREX exon near the center of the 423 bp shared sequence. Once adequate resolution was achieved, measuring and modeling experiments indicated that duplexing between STREX and ZERO strands was almost indiscriminate, and no reliable protocol to eliminate heteroduplexing was found. Others have quantified similar heteroduplexed DNA and reallocated it proportionately (McCulloch et al., 1995; Hayward et al., 1998; Serth et al., 1998; Vu et al., 2000). After developing a protocol that satisfactorily eliminated the slower-migrating spurious bands, leaving three, we could get reproducible estimates of the mix by dividing the heteroduplex band equally between STREX and ZERO. However, we sought validation and maximum accuracy over the full range of STREX fractions through denaturing gel electrophoresis.

Denaturing gel electrophoresis is commonly used for sequencing and mutation analysis, however, we required near 100% denaturation, and found it necessary to supersede common practices, both by increasing denaturant concentrations and maintaining the temperature at near boiling. Only PAGE gels could tolerate the heat, but acceptable denaturing agarose gels were achieved by combining formaldehyde and formamide in the gel and formamide in the running buffer. SYBR Gold dye allowed ng level detection of ssDNA, gave lower background, a greater dynamic range, and results that were much more consistent in absolute values than silver staining methods. Non-linearities associated with lane-width variation and overloading could be avoided,

leaving a consistent single-exponential saturation function. Below 100 ng, staining was nearly linear, but severe asymmetry in the error associated with copy number estimates make it better to calibrate the gel for STREX and ZERO amounts with carefully measured absolute standards before estimating relative copy number.

Extrapolating from product ratios back to template ratios is of great interest, but can it be done reliably? Neither a mathematical model nor empirical data that we are aware of directly addresses the possibility that relative amplification efficiency is sensitive to starting ratio of two templates. After assuring that the reactions were in a subsaturating range of cycle number and not sensitive to absolute template abundance, we ran three reaction series with a full range of STREX ratios, and measured templates and products side by side on the same calibrated gels. We conclude that the template:-product relationship is not linear with a constant slope, but consistently well-described by a Boltzmann-like function. With a 1:1 copy ratio, the amplification efficiency of STREX was 78% that of ZERO over 30 cycles (or 98.3% per cycle). However, if one were to assume independence from the starting ratio, one would severely under- and over-estimate STREX on opposite sides of the midpoint. Thus the more abundant template has a significant advantage, presumably resulting from its greater capacity to consume primer and other reagents early in the reaction, and reflecting the finite availability of those reagents even during the 'linear' portion of the reaction. The precise relationship will be unique for each compound reaction situation and cycle number, but consistent enough to allow very reliable back-extrapolation, despite substantial differences in amplification efficiency.

Our studies demonstrate that the reproducibility of the RT-PCR amplification and quantification is, in this case of dual native templates that are inherently unequal in length, sufficiently good that real inter-individual variation, rather than measurement error, is likely to determine the minimal sample number needed to prove differences. We have also amplified Slo mRNA from single cells, and the results suggest that quantitative accuracy can be achieved even at this level. Similarly accurate quantification should be achievable in other less than ideal multiplex PCR reactions, including those involving two primer pairs targeting unrelated templates. More accurate quantification of splice variant expression in small amounts of tissue should improve our understanding of still largely unidentified regulatory mechanisms, and their potential significance for functional changes in the brain. Better quantification should also encourage the use of transgenes designed with appropriate primer binding sites for calibration against other genes of related interest.

Acknowledgements

This work was supported by NIH RO1 NS40790-01.

References

Apostolakos MJ, Schuermann WH, et al. Measurement of gene expression by multiplex competitive polymerase chain reaction. Anal Biochem 1993;213(2):277–84.

Brenner R, Perez GJ, et al. Vasoregulation by the beta1 subunit of the calcium-activated potassium channel. Nature 2000;407(6806):870–6.

Bustin SA. Absolute quantification of mRNA using real-time reverse transcription polymerase chain reaction assays. J Mol Endocrinol 2000;25(2):169–93.

Diviacco S, Norio P, et al. A novel procedure for quantitative polymerase chain reaction by coamplification of competitive templates. Gene 1992;122(2):313–20.

Gottlieb M, Chavko M. Silver staining of native and denatured eucaryotic DNA in agarose gels. Anal Biochem 1987;165(1):33–7.

Hayward AL, Oefner PJ, et al. Modeling and analysis of competitive RT-PCR. Nucleic Acids Res 1998;26(11):2511–8.

Ingle JD, Crouch SR. Spectrochemical Analysis. Prentice Hall, 1988.

Jung R, Soondrum K, et al. Quantitative PCR. Clin Chem Lab Med 2000;38(9):833–6.

Lai G, McCobb DP. Differential regulation of alternative splicing of the Slo gene by steroid hormones, 2001 submitted.

Lai G, McCobb DP. Opposing actions of glucocorticoids and androgens on alternative splicing of Slo potassium channels in bovine adrenal chromaffin cells. 2002; in press.

Lovell PV, McCobb DP. Pituitary control of BK potassium channel function and intrinsic firing properties of adrenal chromaffin cells. J Neurosci 2001;21(10):3429–42.

Mahmoud SF. Laser-induced fluorescence instrumentation and measurements of dityrosine. In: Chemistry and Biochemistry. Logan, UT: Utah State University, 1994.

Mahmoud SF, Yu Y, et al. Regulation of Slo potassium channel alternative splicing in pituitary by testosterone. 2002; in preparation.

McCobb D. Towards a natural history of calcium-activated potassium channels. Molecular insights into ion channel biology in health and disease. R.A. Maue. Amsterdam, Elsevier Science, 2002 in press.

McCulloch RK, Choong CS, et al. An evaluation of competitor type and size for use in the determination of mRNA by competitive PCR. PCR Methods Appl 1995;4(4):219–26.

Meera P, Wallner M, et al. Molecular biology of high-conductance, Ca^{2+}-activated potassium channels. In: Potassium Channels in Cardiovascular Biology (Chapter 4). A.A. Rusch, Kluwer Academic/Plenum, 2001:49–70.

Ramanathan K, Michael TH, et al. A molecular mechanism for electrical tuning of cochlear hair cells. Science 1999;283(5399):215–7.

Saito M, Nelson C, et al. A cysteine-rich domain defined by a novel exon in a Slo variant in rat adrenal chromaffin cells and PC12 cells. J Biol Chem 1997;272(18):11710–7.

Serth J, Panitz F, et al. Single-tube nested competitive PCR with homologous competitor for quantitation of DNA target sequences: theoretical description of heteroduplex formation, evaluation of sensitivity, precision and linear range of the method. Nucleic Acids Res 1998;26(19):4401–8.

Tian L, Duncan RR, et al. Alternative splicing switches potassium channel sensitivity to protein phosphorylation. J Biol Chem 2001;276(11):7717–20.

Tuma RS, Beaudet MP, et al. Characterization of SYBR Gold nucleic acid gel stain: a dye optimized for use with 300-nm ultraviolet transilluminators. Anal Biochem 1999;268(2):278–88.

Vu HL, Troubetzkoy S, et al. A method for quantification of absolute amounts of nucleic acids by (RT)-PCR and a new mathematical model for data analysis. Nucleic Acids Res 2000;28(7):E18.

Xie J, Black DL. A CaMK IV responsive RNA element mediates depolarization-induced alternative splicing of ion channels. Nature 2001;410(6831):936–9.

Xie J, McCobb DP. Control of alternative splicing of potassium channels by stress hormones, Science 1998;280(443–446).

Yakubovskaya MG, Neschastnova AA, et al. Interaction of linear homologous DNA duplexes via Holliday junction formation. Eur J Biochem 2001;268(1):7–14.